CDF note 8388

Measurement of the Inclusive Jet Cross Section using the k_T algorithm in $p\overline{p}$ Collisions at $\sqrt{s} = 1.96$ TeV

(CDF Collaboration)

(Dated: July 19, 2006)

We present new preliminary results on inclusive jet production as a function of the jet transverse momentum in $p\overline{p}$ collisions at $\sqrt{s} = 1.96$ TeV using data collected with the upgraded Collider Detector at Fermilab in Run II, corresponding to an integrated luminosity of 0.98 fb^{-1}. The measurements are carried out in five different jet rapidity regions for jets with $|y^{\mathrm{jet}}| < 2.1$ and transverse momentum in the range $54 < p_T^{\mathrm{jet}} < 700$ GeV/c. Next-to-leading order perturbative QCD predictions are in good agreement with the measured cross sections after the necessary non-perturbative parton-to-hadron corrections are included.

I. INTRODUCTION

The measurement of the inclusive jet cross section as a function of the jet transverse momentum, p_T^{jet}, in $p\overline{p}$ collisions at $\sqrt{s} = 1.96$ TeV constitutes a test of perturbative QCD (pQCD) [1] predictions over more than eight orders of magnitude in cross section. The increased center-of-mass energy and integrated luminosity in Run II at the Tevatron have allowed to measure the jet cross section for jets with transverse momentum up to about 700 GeV/c, thus extending the p_T^{jet} range by more than 150 GeV/c compared to Run I. In particular, the CDF experiment recently published results [2] on inclusive jet production using the k_T algorithm [3, 4] for jets with $p_T^{\mathrm{jet}} > 54$ GeV/c and rapidity [5] in the region $0.1 < |y^{\mathrm{jet}}| < 0.7$, which are well described by NLO pQCD predictions [6]. This letter presents new measurements of the inclusive jet production cross section as a function of p_T^{jet} in five different jet rapidity regions up to $|y^{\mathrm{jet}}| = 2.1$, using the k_T algorithm and based on 0.98 fb^{-1} of CDF Run II data. The measurements are corrected to the hadron level [7] and compared to pQCD NLO predictions.

II. JET RECONSTRUCTION

The k_T algorithm is used to reconstruct jets in data and Monte Carlo simulated events (see below) from the energy depositions in the calorimeter towers with transverse momentum above 0.1 GeV/c. First, all towers are considered as protojets. The quantities

$$k_{T,i} = p_{T,i}^2 \quad ; \quad k_{T,(i,j)} = \min(p_{T,i}^2, p_{T,j}^2) \cdot \Delta R_{i,j}^2 / D^2, \tag{1}$$

are computed for each protojet and pair of protojets respectively, where $p_{T,i}$ denotes the transverse momentum of the i^{th} protojet, $\Delta R_{i,j}$ is the distance ($y - \phi$ space) between each pair of protojets, and D is a parameter that approximately controls the size of the jet. All $k_{T,i}$ and $k_{T,(i,j)}$ values are then collected into a single sorted list. In this combined sorted list, if the smallest quantity is of the type $k_{T,i}$, the corresponding protojet is promoted to be a jet and removed from the list. Otherwise, if the smallest quantity is of the type $k_{T,(i,j)}$, the protojets are combined into a single protojet by summing up their four-vector components. The procedure is iterated over protojets until the list is empty. The jet transverse momentum, rapidity, and azimuthal angle are denoted as $p_{T,CAL}^{jet}$, y_{CAL}^{jet}, and ϕ_{CAL}^{jet}, respectively. The same jet algorithm is applied to the final-state particles in the Monte Carlo event samples to search for jets at the hadron level. In this case, no cut on the minimum transverse momentum of the particles is applied. The resulting hadron-level jet variables are denoted as $p_{T,HAD}^{jet}$, y_{HAD}^{jet}, and ϕ_{HAD}^{jet}.

III. EVENT SELECTION

The measurements presented in this article correspond to a total integrated luminosity of 0.98 ± 0.06 fb^{-1} of data collected by the CDF experiment in Run II. The CDF II detector is described in detail in [8]. Events were selected *online* using three-level trigger paths, based on the measured energy deposits in the calorimeter towers, with several different thresholds on the jet transverse energies and different prescales. In the first-level trigger, a single trigger tower with transverse energy above 5 GeV or 10 GeV, depending on the trigger path, is required. In the second-level trigger, a hardware-based clustering is carried out where calorimeter clusters are formed around the selected trigger towers. The events are required to have at least one second-level trigger cluster with transverse energy above a given threshold, which varies between 15 and 90 GeV for the different trigger paths. In the third-level trigger, jets are reconstructed using the CDF Run I cone algorithm [9] and the events are required to have at least one jet with transverse energy above 20 to 100 GeV depending on the trigger path. Jets are then searched for using the k_T algorithm with $D = 0.7$. For each trigger data sample, the threshold on the minimum $p_{T,CAL}^{jet}$ is chosen in such a way that the trigger selection is fully efficient and the corresponding prescale is taken into account. The following selection criteria has been imposed:

- The events are selected to have at least one reconstructed primary vertex with z-position within 60 cm around the nominal interaction point.
- Events are required to have at least one jet with rapidity in the region $|y_{CAL}^{jet}| < 2.1$ and corrected transverse momentum (see below) above 54 GeV/c.
- In order to remove beam-related backgrounds and cosmics rays, the events are required to fulfill $\not{E}_T/\sqrt{\Sigma E_T} < F(p_{T,CAL}^{\text{leading jet}})$, where $\not{E}_T$ denotes the missing transverse energy [10] and $\Sigma E_T = \sum_i E_T^i$ is the total transverse energy of the event, as measured using calorimeter towers with E_T^i above 0.1 GeV. The threshold function $F(p_{T,CAL}^{\text{leading jet}})$ is defined as $F(p_T^{jet}) = \min(2 + 0.0125 \times p_T^{jet}, 7)$, where $p_{T,CAL}^{\text{leading jet}}$ is the uncorrected transverse momentum of the leading jet (highest p_T^{jet}) and the units are GeV. This criterion is designed to preserve more than 95% of the QCD events, as determined from Monte Carlo studies. A visual scan for $p_{T,CAL}^{jet} > 400$ GeV/c showed no remaining backgrounds.

Measurements are carried out in five different y_{CAL}^{jet} regions: $|y_{CAL}^{jet}| < 0.1$, $0.1 < |y_{CAL}^{jet}| < 0.7$, $0.7 < |y_{CAL}^{jet}| < 1.1$, $1.1 < |y_{CAL}^{jet}| < 1.6$, and $1.6 < |y_{CAL}^{jet}| < 2.1$, where the different boundaries are dictated by the layout of the CDF calorimeter system. The measurements are limited to jets with $|y_{CAL}^{jet}| < 2.1$ to avoid contributions from the proton/antiproton remnants that would affect the measured $p_{T,CAL}^{jet}$ in the most forward region of the calorimeter.

IV. EFFECT OF MULTIPLE $P\overline{P}$ INTERACTIONS

The measured jet transverse momentum includes additional contributions from multiple proton-antiproton interactions per bunch crossing at high instantaneous luminosity. The data used in this measurement were collected at Tevatron instantaneous luminosities between $0.2 \times 10^{31}\text{cm}^{-2}\text{s}^{-1}$ and $16.3 \times 10^{31}\text{cm}^{-2}\text{s}^{-1}$ with an average of $4.1 \times 10^{31}\text{cm}^{-2}\text{s}^{-1}$, for which, in average, 1.5 inelastic proton-antiproton interactions per bunch crossing are expected. At the highest instantaneous luminosities considered, an average of 5.9 interactions per bunch crossing are produced. This mainly affects the measured cross section at low p_T^{jet} where the contributions are sizeable. In CDF, multiple interactions are identified via the presence of additional primary vertices reconstructed from charged particles. The measured jet transverse momenta are corrected for this effect by removing a certain amount of transverse momentum, ϵ, for each additional primary vertex, as determined from the data by requiring that, after the correction is applied, the ratio of cross sections at low and high instantaneous luminosities does not show any p_T^{jet} dependence. The study is carried out separately in each y_{CAL}^{jet} region, and the results are consistent with a common value $\epsilon = 1.62^{+0.70}_{-0.46}$ GeV/c across the whole rapidity range.

V. MONTE CARLO SIMULATION

Monte Carlo event samples are used to determine the response of the detector and the correction factors to the hadron level. The generated samples are passed through a full CDF detector simulation (based on GEANT3 [11] where the GFLASH [12] package is used to simulate the energy deposition in the calorimeters) and then reconstructed and analyzed using the same analysis chain as in the data. Samples of simulated inclusive jet events have been generated using PYTHIA 6.203 [13] and HERWIG 6.4 [14] Monte Carlo generators. CTEQ5L [15] parton distribution functions are used for the proton and antiproton. The PYTHIA samples have been created using a special tuned set of parameters, denoted as PYTHIA-TUNE A [16], that includes enhanced contributions from initial-state gluon radiation and secondary parton interactions between remnants. TUNE A was determined as a result of dedicated studies of the underlying event using the CDF Run I data [17] and has been shown to properly describe the measured jet shapes in Run II [18]. In the case of PYTHIA, fragmentation into hadrons is carried out using the string model [19] as implemented in JETSET [20], while HERWIG implements the cluster model [21].

VI. UNFOLDING

The measured $p_{T,CAL}^{jet}$ distributions in the different $|y_{CAL}^{jet}|$ regions are unfolded back to the hadron level using Monte Carlo event samples. PYTHIA-TUNE A provides a reasonable description of the different jet and underlying event quantities, and is used to determine the correction factors in the unfolding procedure. In order to avoid any bias on the correction factors due to the particular PDF set used during the generation of the Monte Carlo samples, which translates into slightly different simulated $p_{T,CAL}^{jet}$ distributions, PYTHIA-TUNE A is re-weighted until it accurately follows each of the measured $p_{T,CAL}^{jet}$ distributions.

The unfolding is carried out in two steps. First, an average correction is computed separately in each jet rapidity region using matched pairs of jets at the calorimeter and hadron levels. The correlation $< p_{T,HAD}^{jet} - p_{T,CAL}^{jet} >$ vs

$< p^{\rm jet}_{\rm T,CAL} >$, computed in bins of $(p^{\rm jet}_{\rm T,HAD} + p^{\rm jet}_{\rm T,CAL})/2$, is used to extract correction factors which are then applied to the measured jets to obtain the corrected transverse momenta, $p^{\rm jet}_{\rm T,COR}$. In each jet rapidity region, a raw cross section is defined as

$$\frac{d^2\sigma}{dp^{\rm jet}_{\rm T,COR}dy^{\rm jet}_{\rm CAL}} = \frac{1}{\mathcal{L}}\frac{N^{\rm jet}_{\rm COR}}{\Delta p^{\rm jet}_{\rm T,COR}\ \Delta y^{\rm jet}_{\rm CAL}}, \tag{2}$$

where $N^{\rm jet}_{\rm COR}$ denotes the number of jets in a given $p^{\rm jet}_{\rm T,COR}$ bin, $\Delta p^{\rm jet}_{\rm T,COR}$ is the size of the bin, $\Delta y^{\rm jet}_{\rm CAL}$ denotes the size of the considered region in $y^{\rm jet}_{\rm CAL}$, and $\mathcal{L}$ is the integrated luminosity. Second, each measurement is corrected for acceptance and smearing effects using a bin-by-bin unfolding procedure, which also accounts for the efficiency of the selection criteria. The unfolding factors, defined as

$$U(p^{\rm jet}_{\rm T,COR}, y^{\rm jet}_{\rm CAL}) = \frac{d^2\sigma/dp^{\rm jet}_{\rm T,HAD}dy^{\rm jet}_{\rm HAD}}{d^2\sigma/dp^{\rm jet}_{\rm T,COR}dy^{\rm jet}_{\rm CAL}}, \tag{3}$$

are extracted from Monte Carlo event samples and applied to the measured $p^{\rm jet}_{\rm T,COR}$ distributions to obtain the final results. The factor $U(p^{\rm jet}_{\rm T,COR}, y^{\rm jet}_{\rm CAL})$ increases with $p^{\rm jet}_{\rm T,COR}$ and shows a moderate $y^{\rm jet}_{\rm CAL}$-bin dependence. At very low $p^{\rm jet}_{\rm T,COR}$, the unfolding factor varies between 1.02 and 1.06 for different rapidity regions. For jets with $p^{\rm jet}_{\rm T,COR}$ about 300 GeV/c, the factor varies between 1.1 and 1.2, and increases up to 1.3 - 1.4 at very high $p^{\rm jet}_{\rm T,COR}$.

VII. SYSTEMATIC UNCERTAINTIES

A detailed study of the systematic uncertainties on the measurements was carried out [2, 22]. The total systematic uncertainty on the different measurements is dominated by the uncertainty on the absolute jet energy scale. The measured jet energies were varied by ±2% at low $p^{\rm jet}_{\rm T}$ to ±3% at high $p^{\rm jet}_{\rm T}$. This introduces an uncertainty on the measured cross sections which varies between ±9% at low $p^{\rm jet}_{\rm T}$ and $^{+60\%}_{-40\%}$ at high $p^{\rm jet}_{\rm T}$. Other sources of systematic uncertainty include: a ±8% uncertainty on the jet energy resolution, the Monte Carlo simulation of the jet energy response in partially instrumented regions of the calorimeter, the model for parton shower and hadronization employed in the unfolding, a possible residual dependence on the $p^{\rm jet}_{\rm T}$ spectra in the computed unfolding factors, and the quoted uncertainty on ϵ. Systematic uncertainties related to the selection criteria were found to contribute less than 2% to the total systematic uncertainty. The uncertainty on the integrated luminosity is 5.8%.

VIII. RESULTS

The measured inclusive jets cross sections, $\frac{d^2\sigma}{dp_T^{jet} dy^{jet}}$, refer to hadron level jets, reconstructed using the k_T algorithm with $D = 0.7$, in the region $p_T^{jet} > 54$ GeV/c and $|y^{jet}| < 2.1$. Figure 1 shows the measured cross sections as a function of p_T^{jet} in five different $|y^{jet}|$ regions compared to NLO pQCD predictions where, for presentation, each measurement has been scaled by a given factor. The measured cross sections decrease by more than seven to eight orders of magnitude as p_T^{jet} increases. The NLO pQCD predictions are computed using JETRAD [6] with CTEQ6.1M PDFs [24] and the renormalization and factorization scales (μ_R and μ_F) set to $\mu_0 = \max(p_T^{jet})/2$.

Different sources of uncertainty in the theoretical predictions were considered. The main contribution comes from the uncertainty on the PDFs and was computed using the Hessian method [25]. At low p_T^{jet} the uncertainty is about $\pm 5\%$ and approximately independent of y^{jet}. The uncertainty increases as p_T^{jet} and y^{jet} increase. At very high p_T^{jet}, the uncertainty varies between $^{+60\%}_{-30\%}$ and $^{+130\%}_{-40\%}$ for jets with $|y^{jet}| < 0.1$ and $1.6 < |y^{jet}| < 2.1$, respectively, and is dominated by the limited knowledge of the gluon PDF. An increase of μ_R and μ_F from μ_0 to $2\mu_0$ reduces the theoretical predictions by 2% at low p_T^{jet} and 8% at high p_T^{jet}. Values significantly smaller than μ_0 lead to unstable NLO results and were not considered.

The theoretical predictions include a correction factor, $C_{HAD}(p_T^{jet}, y^{jet})$, that approximately accounts for non-perturbative contributions from the underlying event and fragmentation into hadrons (see Figure 2). In each jet rapidity region, C_{HAD} was estimated, using PYTHIA-TUNE A, as the ratio between the nominal $p_{T,HAD}^{jet}$ distribution and the one obtained by turning off both the interactions between proton and antiproton remnants and the fragmentation in the Monte Carlo samples. The correction decreases as p_T^{jet} increases and shows a moderate y^{jet} dependence. At low p_T^{jet}, C_{HAD} varies between 1.18 and 1.13 as y^{jet} increases, and it becomes of the order of 1.02 at very high p_T^{jet}. The uncertainty on C_{HAD} varies between 9% and 12% at low p_T^{jet} and decreases down to about 1% at very high p_T^{jet}, as determined from the difference between the parton-to-hadron correction factors obtained using HERWIG instead of PYTHIA-TUNE A.

Figure 3 shows the ratios data/theory as a function of p_T^{jet} in the five different $|y^{jet}|$ regions. Good agreement is observed in the whole range in p_T^{jet} and y^{jet} between the measured cross sections and the theoretical predictions. In particular, no significant deviation from the pQCD prediction is observed for central jets at high p_T^{jet}. In the most forward region, the uncertainty on the theoretical prediction at high p_T^{jet} is larger than that on the measured cross section, which indicates that the data presented in this letter will contribute to a better understanding of the gluon PDF. In addition, Figure 3 shows the ratio of pQCD predictions using MRST2004 [26] and CTEQ6.1M PDF sets.

IX. SUMMARY AND CONCLUSIONS

In summary, we have presented preliminary results on inclusive jet production in $p\bar{p}$ collisions at $\sqrt{s} = 1.96$ TeV using the $\mathrm{k_T}$ algorithm, for jets with transverse momentum $\mathrm{p_T^{jet}} > 54$ GeV/c and rapidity in the region $|\mathrm{y^{jet}}| < 2.1$, based on 0.98 fb^{-1} of CDF Run II data. The measured cross sections are in agreement with NLO pQCD predictions after the necessary non-perturbative parton-to-hadron corrections are taken into account. The data presented in this letter will contribute to a better understanding of the gluon PDF in the proton.

Acknowledgments

We thank the Fermilab staff and the technical staffs of the participating institutions for their vital contributions. This work was supported by the U.S. Department of Energy and National Science Foundation; the Italian Istituto Nazionale di Fisica Nucleare; the Ministry of Education, Culture, Sports, Science and Technology of Japan; the Natural Sciences and Engineering Research Council of Canada; the National Science Council of the Republic of China; the Swiss National Science Foundation; the A.P. Sloan Foundation; the Bundesministerium fuer Bildung und Forschung, Germany; the Korean Science and Engineering Foundation and the Korean Research Foundation; the Particle Physics and Astronomy Research Council and the Royal Society, UK; the Russian Foundation for Basic Research; the Comision Interministerial de Ciencia y Tecnologia, Spain; in part by the European Community's Human Potential Programme under contract HPRN-CT-2002-00292; and the Academy of Finland.

---

[1] D.J. Gross and F. Wilczek, Phys. Rev. D **8**, 3633 (1973).
H.Fritzsch, M. Gell-Mann and H. Leutwyler, Phys. Lett. **B47**, 365 (1973).

[2] A. Abulencia *et al.* (CDF Collaboration), Phys. Rev. Lett. **96**, 122001 (2006).

[3] S. Catani *et al.*, Nucl. Phys. B **406**, 187 (1993).

[4] S.D. Ellis and D.E. Soper, Phys. Rev. D **48**, 3160 (1993).

[5] We use a cylindrical coordinate system about the beam axis in which θ is the polar angle and ϕ is the azimuthal angle. We define $E_T = E\ \sin\theta$, $p_T = p\ \sin\theta$, $\eta = -\ln(\tan(\frac{\theta}{2}))$, and $y = \frac{1}{2}\ln(\frac{\mathrm{E+p_z}}{\mathrm{E-p_z}})$.

[6] W.T. Giele, E.W.N. Glover and David A. Kosower, Nucl. Phys. B **403**, 633 (1993).

[7] The hadron level in the Monte Carlo generators is defined using all final-state particles with lifetime above 10^{-11}s.

[8] D. Acosta *et al.* (CDF Collaboration), Phys. Rev. D **71**, 032001 (2005).

[9] CDF Collab., F. Abe et al.,Phys. Rev. D **45**, 1448 (1992).

[10] $\not\!\!E_T$ is defined as the norm of $-\sum_i E_T^i \cdot \vec{n}_i$, where $\vec{n}_i$ is the unit vector in the azimuthal plane that points from the beamline to the i-th calorimeter tower.

[11] R. Brun *et al.*, Tech. Rep. CERN-DD/EE/84-1, 1987.

[12] G. Grindhammer, M. Rudowicz and S. Peters, Nucl. Instrum. Meth. A **290**, 469 (1990).

[13] T. Sjöstrand *et al.*, Comp. Phys. Comm. **135**, 238 (2001).

[14] G. Corcella *et al.*, JHEP **0101**, 010 (2001).

[15] H.L. Lai *et al.*, Eur. Phys. J. C **12**, 375 (2000).

[16] PYTHIA-Tune A Monte Carlo samples are generated using the following tuned parameters in PYTHIA: PARP(67) = 4.0, MSTP(82) = 4, PARP(82) = 2.0, PARP(84) = 0.4, PARP(85) = 0.9, PARP(86) = 0.95, PARP(89) = 1800.0, PARP(90) = 0.25.

[17] T. Affolder *et al.* (CDF Collaboration), Phys. Rev. D **65**, 092002 (2002).

[18] D. Acosta *et al.* (CDF Collaboration), Phys. Rev. D **71**, 112002 (2005).

[19] B. Andersson *et al.*, Phys. Rep. **97**, 31 (1983).

[20] T. Sjöstrand, Comp. Phys. Comm. **39**, 347 (1986).

[21] B.R. Webber, Nucl. Phys. B **238**, 492 (1984).

[22] Olga Norniella, PhD. Thesis, Universitat Autónoma de Barcelona, in preparation.

[23] A. Bhatti *et al.*, hep-ex/0510047.

[24] J. Pumplin *et al.*, JHEP **0207**, 012 (2002).

[25] J. Pumplin *et al.*, Phys. Rev. D **65**, 014013 (2002).

[26] A. D. Martin *et al.*, Eur. Phys. J. C **23**, 73 (2002).

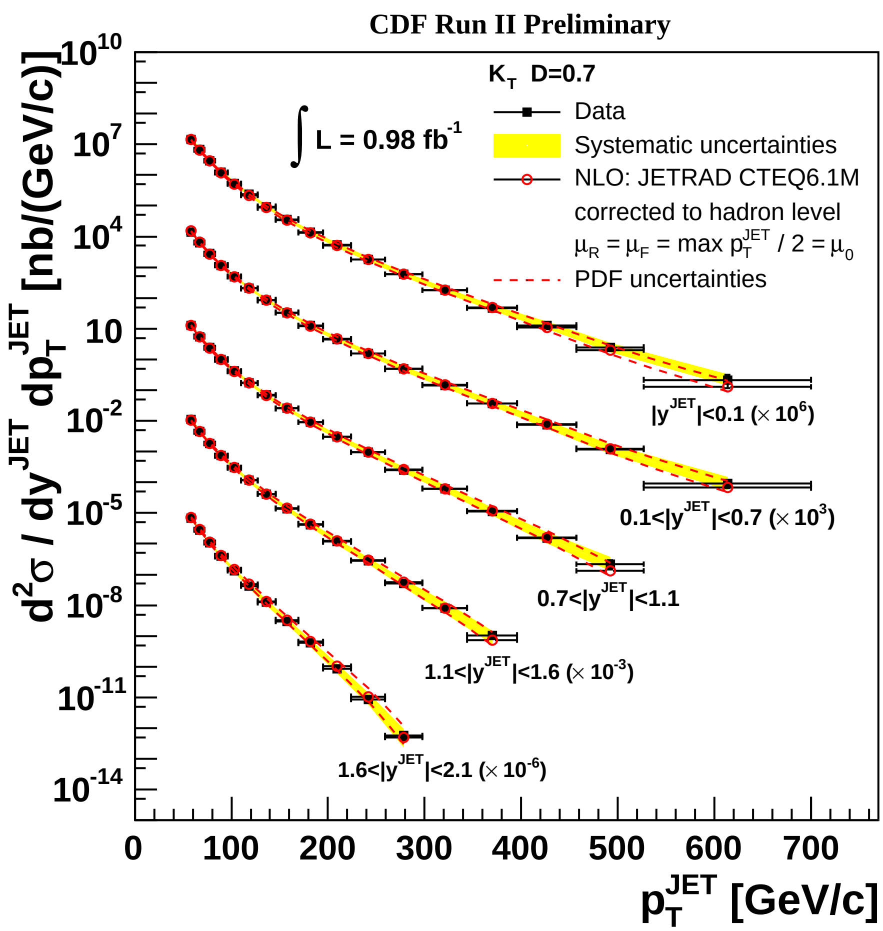

FIG. 1: Measured inclusive jet cross sections (filled squares) as a function of p_T^{jet} for jets with $p_T^{jet} > 54$ GeV/c in different y^{jet} regions compared to NLO pQCD predictions (open circles). The shaded band shows the total systematic uncertainty on the measurement. A 5.8% uncertainty on the luminosity is not included. The dashed lines indicate the PDF uncertainty on the theoretical predictions. For presentation, each measurement is scaled by a given factor.

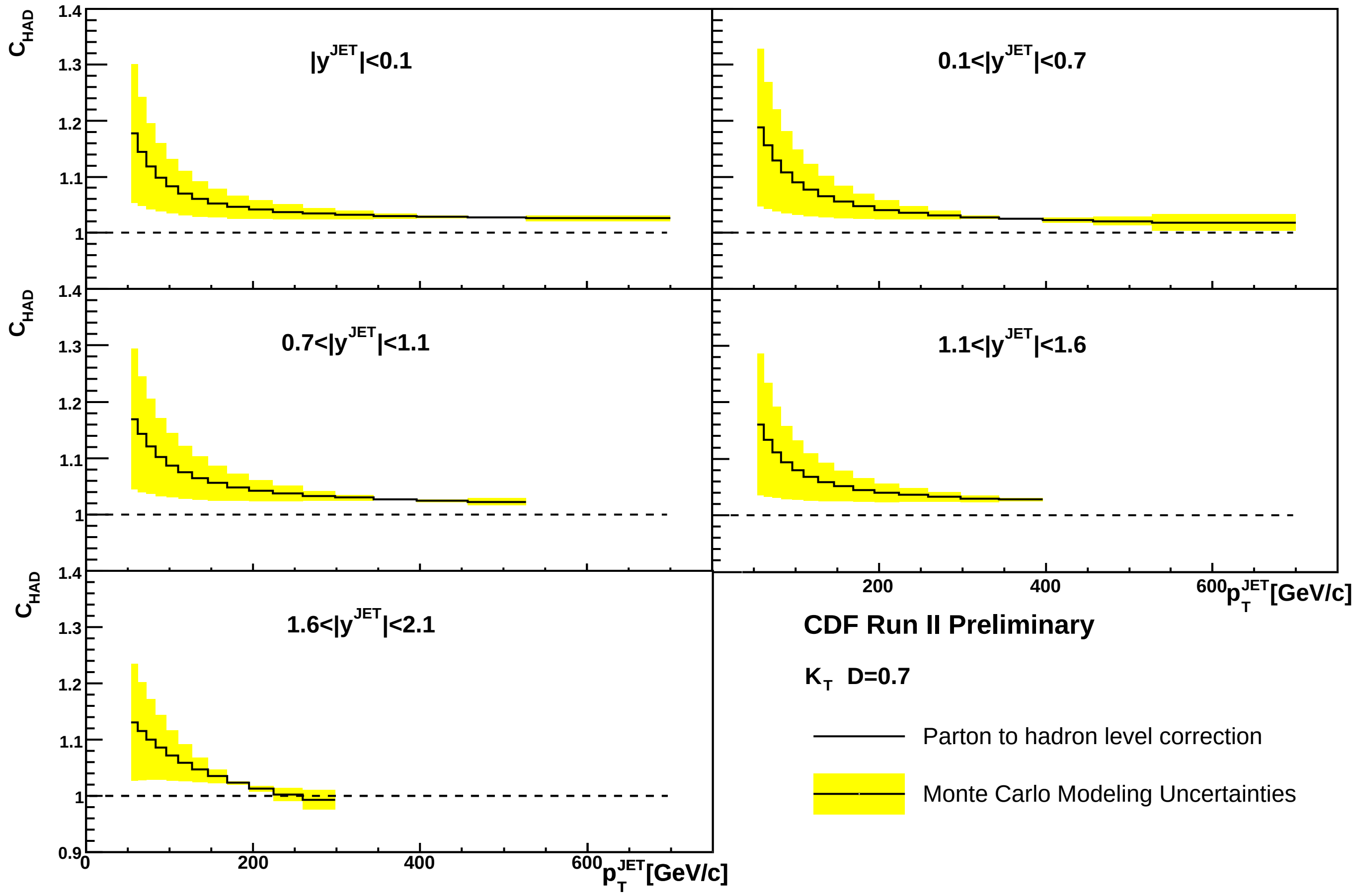

FIG. 2: Magnitude of the parton-to-hadron correction, $C_{\rm HAD}(\mathrm{p_T^{jet}}, \mathrm{y^{jet}})$, used to correct the NLO pQCD predictions. The shaded band indicates the quoted Monte Carlo modeling uncertainty.

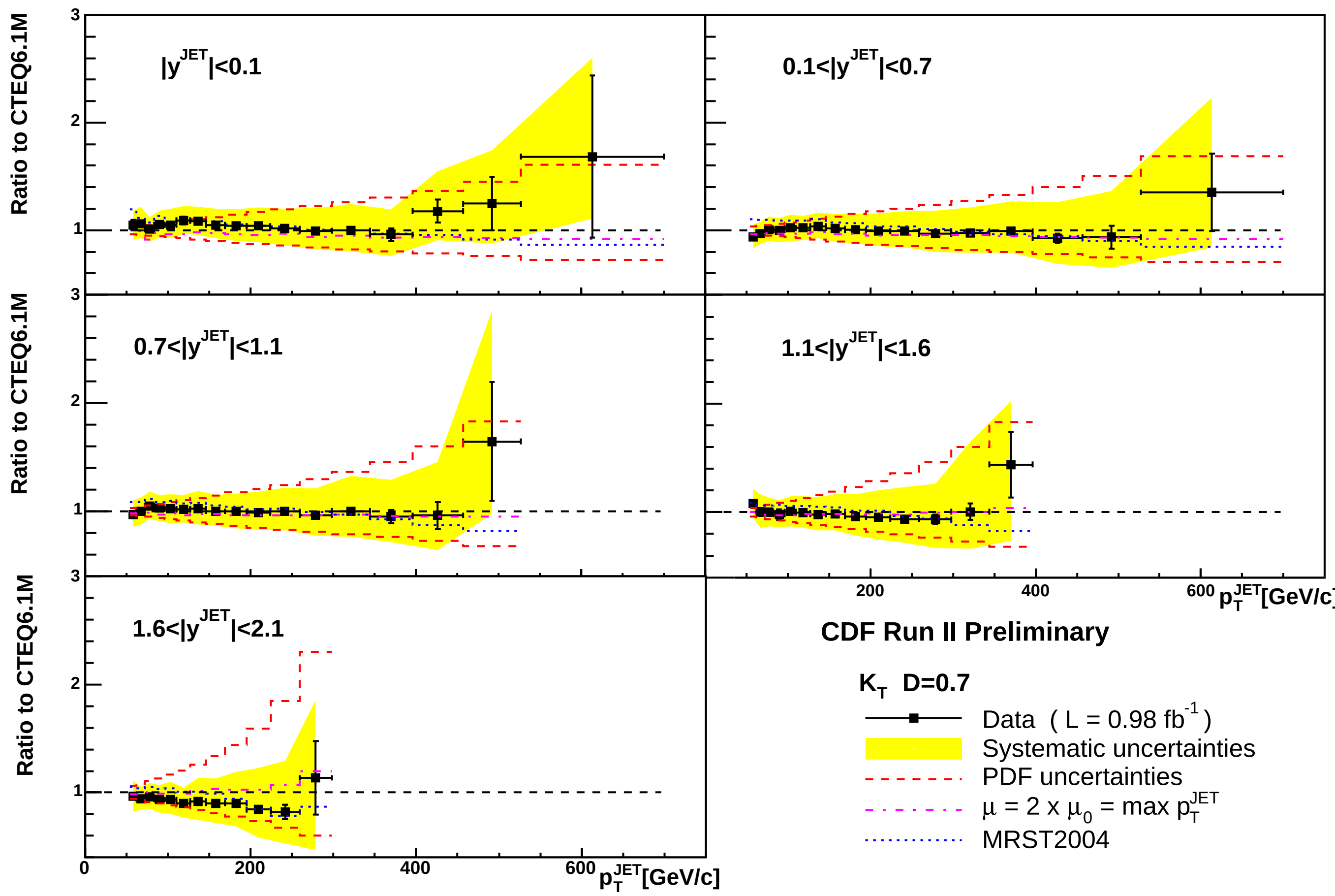

FIG. 3: Ratio Data/Theory as a function of p_T^{jet} in different $|y^{jet}|$ regions. The error bars (shaded band) show the total statistical (systematic) uncertainty on the data. A 5.8% uncertainty on the luminosity is not included. The dashed lines indicate the PDF uncertainty on the theoretical prediction. The dotted line presents the ratio of MRST2004 and CTEQ6.1M predictions. The dotted-dashed line shows the ratio of predictions with $2\mu_0$ and μ_0.